Distribution of parameters
of elliptic approximation
of the human pupil

Marta A. SZMIGIEL*, Henryk KASPRZAK

Department of Optics and Photonics, Faculty of Fundamental Problems of Technology,
Wrocław University of Technology, Wybrzeże Wyspiańskiego 27, 50-370 Wrocław, Poland

*Corresponding author: Marta.Szmigiel@pwr.edu.pl

The paper describes the results of measurements of the shape of the human eye pupil with the use of a high-speed CCD camera. Sequences of 2000 frames were recorded within 10 s. The examination was performed on a group of patients. For each patient, the age and intraocular pressure were identified. The form of the pupil was approximated by an ellipse and parameters of area, eccentricity, lengths of semi axes and orientation angle were calculated. Correlations between pairs of averaged parameters for all measurements were analyzed. Distribution of averaged geometrical parameters of the pupil was examined for all measured pupils. Significant correlation was found between the age and the pupil area S. The average eccentricity ε of the pupil was 0.285 ± 0.083. There were no statistical differences between pupil eccentricities of both eyes. The average value of orientation angle α of the longer semi-axis a of the ellipse to horizon was 83.3°. Also the difference of orientation angle α for the left eye (85.2°) and the right eye (93.2°) was statistically insignificant.

Keywords: pupil of the eye, pupil parameters, pupil approximation.

1. Introduction

The iris is a multi-layered structure [1] with the pupil located in its center. The size and the shape of the pupil is associated with the action of two independent muscles. The dilator muscle is stimulated by the sympathetic nervous system and makes the pupil widen. The iris sphincter muscles are stimulated by the parasympathetic nervous system and cause narrowing of the diameter of the pupil. Since these two muscles are stimulated by different nervous systems, the dynamics of the pupil size and geometry is a complex process.

The iris pupil plays an important role in the optical system of the eye. Due to the geometry and size variability it affects not only the amount of light illuminating the retina but also the eye aberrations and form of the point spread function (PSF) of

the eye. Thus, the form and size of the pupil influence directly the quality of the retinal image. When the pupil of the eye expands, the effect of diffraction reduces and PSF becomes more narrow. At the same time, eye aberrations play more important role. Therefore some optimal size of the eye pupil exists, which ensures the highest eye resolution.

On the other hand, the eye pupil is observed and measured through the cornea, which behaves like a magnifying glass. Therefore the real pupil is always smaller, and located in a slightly different position [2]. Additionally, corneal astigmatism may influence the form of the observed pupil. Differences between the real size and form of the pupil in comparison to the observed one depend on the corneal curvature, depth of the anterior chamber and orientation as well as magnitude of the corneal astigmatism. This shows that the quantitative analysis and interpretation of the pupil size and geometry are not a simple task.

The human pupil continuously changes its size and geometry due to many different stimuli. Generally these stimuli can be divided into external and internal ones. The external ones are for example light intensity, a sudden noise, unexpected touch or sight, while the internal can be an emotional state, used drugs or other medicines or agents, the blood pulsing phase, *etc*. The pupil undergoes also small, continuous fluctuations known as hippus [3, 4]. It is also observed that the size of the pupil decreases with age under different light conditions [5, 6].

Pupil geometry and its changes are the subject of research for many years. Pupillometry, measurement of the pupil form, size and its variations, is used to describe sleep disorders [7], reaction to pain [8, 9] or drug metabolism [10, 11]. Moreover, nowadays pupillometry is also used by refractive surgeons before and after refractive surgery – LASIK treatment [12, 13].

Different kinds of pupillometers have been designed. One was based on two lines of CCD sensors [14], which registered spontaneous pupillary fluctuation (SPF) with the frequency of 50 or 90 Hz. Two different pupillometers, static and dynamic, are used by Meeker *et al*. [15]. The dynamic one is equipped with a camera, which records with the frequency of 40 fps. Another pupillometer, a new hand-held point-and-shoot pupillometer (NeurOptics), was used by Olson *et al*. [16], as well as the pupillometer based on an infrared camera, which could record in complete darkness as fast as 50 fps [17].

Images of the pupil recorded with the camera are processed numerically by use of the edge detecting algorithm [18]. In case of the dark iris and black pupil it is more difficult to detect correctly the pupil border. In order to enhance the pupil image, we used infrared illumination and that makes the pupil significantly brighter than the iris.

The first approximation of the shape of the human pupil is a circle [19]. However the pupil is not truly circular [20]. A definitely better approximation of the pupil shape is an ellipse [20–22] with its parameters. Sometimes only "shape parameters" like area, centroid, major and minor axis length, eccentricity and orientation are presented, without fitting the ellipse [18].

Wyatt introduces the concept of noncircularity, which describes how much of the noncircular shape of a given pupil is contributed by the best-fit ellipse [20].

Results of these parameter for 23 subjects were presented for measurements in dark and in the light.

Most of the work shows parameters of the pupil for a few subjects [19]. WINN *et al.* measured one shape parameter only, pupil diameters, of larger group of patients, that is 91 subjects [5], while WYATT of 23 subjects [20]. According to our best knowledge, there are no results on larger numbers of patients, determining the distribution of different geometric parameters of the human pupil. This work presents the parameters of the best fitted ellipse and their distribution, calculated for a group of patients. That gives a possibility to conclude about the dominant values of determined parameters.

2. Method

A system for recording images of the human pupil and its fast variations in time was designed. The main element of the system is a fast AOS S-PRI camera (AOS Technologies AG), capable of recording up to 1250 fps with CCD sensor resolution 800×600 pixels. It is equipped with the Jupiter photo lens 2/85 and the bellow for microphotography, which ensures the optimal image size of the pupil on the image sensor. The camera is located approximately on the axis of sight of the measured eye, to achieve sharp borders of the pupil. The eye illuminator uses 24 near infrared diodes with the wavelength 850 nm.
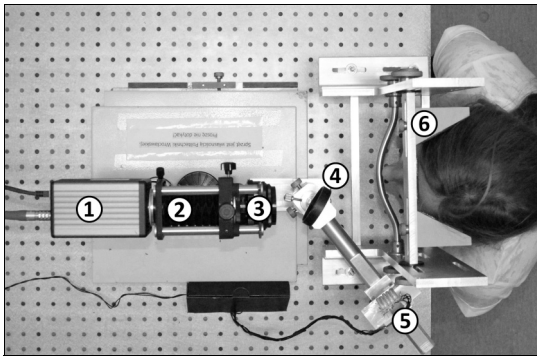

Fig. 1. The scheme of a measuring system for recording the pupil of the eye: 1 – CCD camera, 2 – bellow for microphotography, 3 – lens, 4 – beam splitter, 5 – pupil illuminator, 6 – rigid head rest.

Light from IR diodes is reflected from a beam splitter and illuminates the pupil almost perpendicularly to the iris plane. Thus, one obtains bright reflections from the retina and the contrastive border of the pupil image. Figure 1 presents the scheme of a measuring system.

Since the system is also used to track the position of the pupil center, a special rigid head rest was designed and fabricated. Video sequences were recorded with the frame rate of 200 fps for up to 10 seconds, giving 2000 frames for one measurement. Such a high frame rate in this device is also applicable for testing fast eye movements.
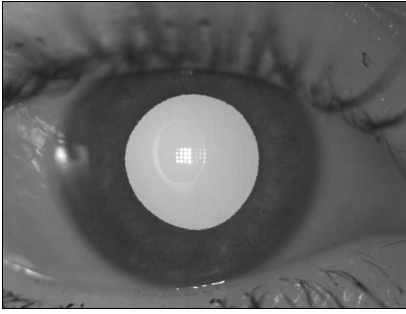
Fig. 2. Image of the pupil.

Figure 2 shows an example of a single image from the sequence. Usually the magnification of recorded and analyzed pupil images was greater in comparison to the exemplary image given in Fig. 2.

The measurements were performed on a group of 55 volunteered patients (84 eyes) in the age of 30 to 81 year old. For each measured eye, one of the recorded sequences has been taken into consideration.

For all the groups, the intraocular pressure (IOP) was measured by use of an air puff tonometer. Three measurements were performed and the average value was taken into account. This measurement was performed 2 to 5 minutes before the pupil examination.

The recorded video sequence was divided into single frames, and each frame was numerically analyzed by use of Matlab software. Selection of border points of the pupil was held automatically, using an edge detection procedure. The shape of the pupil was treated as a filled plane figure. Due to differences in magnification of the pupil, for each sequence, calibration of the pupil size was performed. In each case, when magnification of the camera was changed, the image of a calibration grid was performed. The depth of field in the system was low and constant.

For each separate image from the sequence recorded on the time t, zero order moment, that is the filled pupil area S_t, was determined [23]. Calculations were carried out for the elliptic approximation of the pupil, which fits the ellipse, and has the same second moments as the filled pupil [23]. The lengths a_t and b_t of semi-axes of the ellipse and its eccentricity ε_t were determined, as well as the angle of ellipse orientation in relation to the horizon α_t and the center of the approximated ellipse $(x_{\text{ect}}, y_{\text{ect}})$. Figure 3**a** shows the exemplary image of patient's pupil, with marked parameters of the best fitted ellipse. For some of the patients the shape of the pupil significantly differed from the circle, which is the primary approximation of its shape.

Figures 3**b** and 3**c** present fragments of the border of two different pupils. Differences in the form of the pupil border can be clearly visible. The edges of some pupils are almost smooth (Fig. 3**b**), while others have something we called "flounce" (Fig. 3**c**). Sometimes the pupil "flounce" can be observed as relatively monotonous, in other cases the shape appears to be incidental. Hence for further analysis, the calculated real area of the pupil was taken into consideration, not the area of the approx-
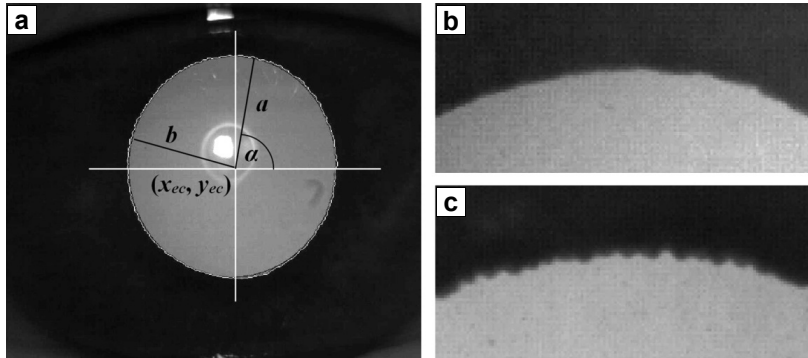
Fig. 3. The pupil of a patient with the fitted ellipse (white line – the shape of the pupil, black line – the shape of the best fitted ellipse, (x_{ec}, y_{ec}) – coordinates of the center of the ellipse, a – large axis, b – small axis, α – the angle of orientation in relation to the horizon) [9] – **a**, and fragments of pupils of different patients – **b**, **c**.

imating ellipse. It can be noticed, however, that the image of the pupil edge is not sharp. As shown in the work of SzczĘsna and Kasprzak [2] off axis aberrations of the cornea (as magnifying glass) limit the resolution capability of the pupil imaging, observed through the cornea.

Figure 4 presents the example of variability of the pupil area S_t and the ellipse eccentricity ε_t within 10 seconds. As it can be observed, there exists some similarity between both curves. This similarity concerns mainly positions of local extremes. This effect occurs also in other patients.

Series of parameters obtained from calculations were treated as raw data and they needed some pre-processing (high pass filtering, removing false peaks, *etc*.) to perform their further analysis. Next, the average values of every ellipse parameters in the whole sequence (10 seconds long) were calculated for each measurement. That means that the parameters S, α, ε and a were determined as mean values with their standard de-
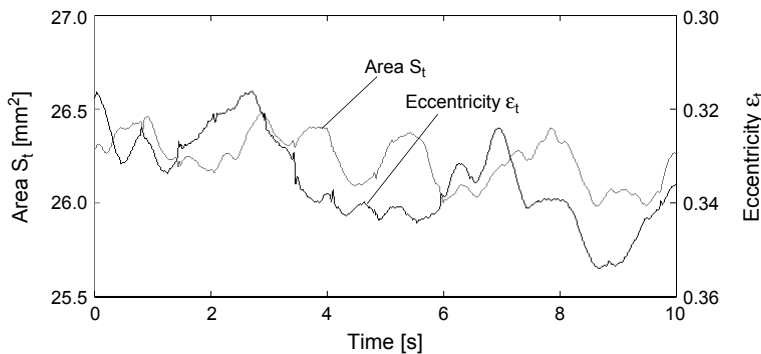

Fig. 4. Time variations of the area S_t and eccentricity ε_t of the pupil within 10 seconds for one patient.

viations from time varying parameters S_t, α_t, ε_t and a_t, respectively. The results of all calculations were compared and analyzed for the whole group of patients.

3. Results

Selected 84 sequences were analyzed, of which 41 were of the right eye and 43 were of the left eye. For further analysis, the parameters describing: the real area of the pupil S (which differs by no more than 0.4% of the area of the best fitted ellipse S_{el}), the angle of orientation in relation to the horizon α, the eccentricity ε and the length of the major semi-axis a were selected.

Also the age of the patients A was taken into account. Table 1 shows selected parameters for the analyzed pupil measurement sequences.

T a b l e 1. The selected parameters for the analyzed pupil measurement sequences.

	RE (mean ± std)	LE (mean ± std)	All (mean ± std)
	Area S [mm^2]		
Average	23.90 ± 8.89	25.84 ± 8.92	26.24 ± 8.90
Min	9.68 ± 0.58	12.62 ± 0.17	9.68 ± 0.58
Max	47.87 ± 1.28	48.26 ± 0.70	48.26 ± 0.70
	Eccentricity ε		
Average	0.280 ± 0.076	0.293 ± 0.089	0.285 ± 0.083
Min	0.135 ± 0.032	0.127 ± 0.023	0.135 ± 0.032
Max	0.478 ± 0.016	0.485 ± 0.001	0.485 ± 0.001
	Angle of orientation α [deg]		
Average	93.20 ± 39.82	85.18 ± 41.37	82.08 ± 40.58
Min	3.60 ± 1.30	19.81 ± 3.73	3.60 ± 1.30
Max	174.27 ± 4.50	179.76 ± 9.29	174.27 ± 19.86
	Age of patient A [years]		
Average	60.8 ± 14.8	59.2 ± 14.3	60.3 ± 14.5
Min	27	30	30
Max	85	74	81

Minimum value is the lowest of the mean in the population, with its standard deviation (std) in the analyzed sequence. Maximum value is the largest value of the mean in the population, with its standard deviation in the analyzed sequence. The average value is the average for all means of the sequences with the standard deviation from the average.

Figure 5 presents the area of the pupil S as a function of age A of a patient. As it was expected [5, 6], it is noticeable that the area of the pupil decreases with age. The mean value of S in the group of octogenarians is 17.7 ± 4.1 mm^2, while in the group of tricenarians is 37.4 ± 10.0 mm^2.

The graph also includes the secondary right axis, defining a circular diameter of the pupil, with the same area as measured for the real pupil.
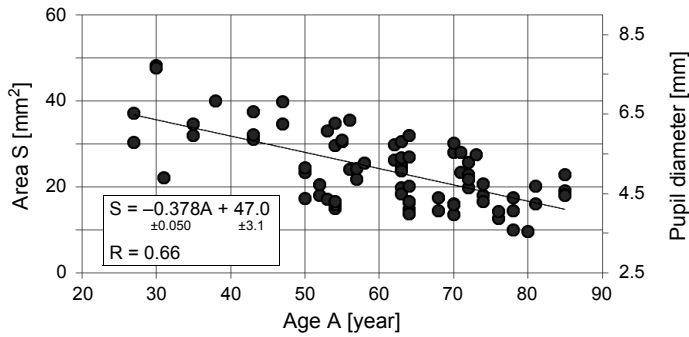
Fig. 5. The area of the pupil *S* as a function of patient's age *A* (additionally, the axis of a pupil diameter added).

The Pearson correlation parameter *R* between all selected parameters was verified. Table 2 presents results for all sequences (in the upper right part of the table), for right eyes only and for left eyes only (in the left bottom of the table, the columns of different gray level background).

T a b l e 2. The Pearson correlation parameter *R* between all selected parameters.

R parameter	*S*		*ε*		*α*		*a*		*A*		IOP
S	–		0.07		0.09		0.99		0.66		0.11
ε	0.08	0.09	–		0.07		0.01		0.09		0.17
α	0.09	0.06	0.09	0.14	–		0.09		0.05		0.17
a	0.99	0.99	0.02	0.00	0.09	0.07	–		0.64		0.14
A	0.65	0.66	0.10	0.09	0.03	0.08	0.65	0.64	–		0.07
IOP	0.08	0.15	0.03	0.40	0.26	0.06	0.08	0.21	0.07	0.09	–

where: ☐ – for all sequences, ■ – for right eyes, ☐ – for left eyes.

It is noticeable that a very high correlation exists between the area *S* and the length of the semi-axis *a*. Also the area *S* is correlated with the age *A*. For the rest of presented parameters, their mutual correlation was relatively small.

In this study, also the distribution of the angle of orientation of major axis in relation to the horizon *α* in the analyzed group was considered, both for all sequences, and having the right and left eye in separate groups. Figure 6 presents the histogram of the orientation angle *α*.

As it is shown in Table 1 and Fig. 6, there is a difference between the mean value of *α* for left and right eyes. Right and left eyes show the difference in orientation of over 8 degrees. With the use of Student's *t*-test, the relevance was verified and the difference in average values for right and left eyes was statistically insignificant.

The distribution of the ellipse eccentricity *ε* in the analyzed group was considered, both for the right and left eye in separate groups. Figure 7 presents the histogram of the eccentricity *ε*.
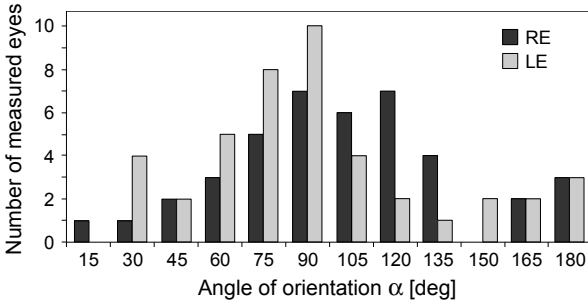
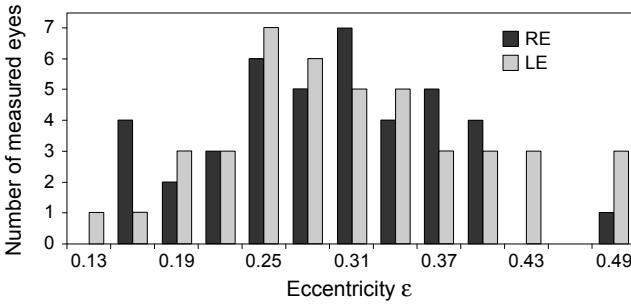Fig. 6. The angle of orientation of the long ellipse axis in relation to the horizon α for right and left eyes.

Fig. 7. The eccentricity ε for all of the right eyes and for all of the left eyes.

The average ε value was 0.282, with standard deviation equal to 0.017. Differences in the values of the right and the left eye pupil ε_L and ε_R had no significance, according to statistical analysis.

Figure 8 presents the dependence of the eccentricity ε and the orientation angle α for the right and left eyes.

It was examined if there is a correlation between the eccentricity ε and the orientation angle α. There was no evidence of such a relationship both for the right and
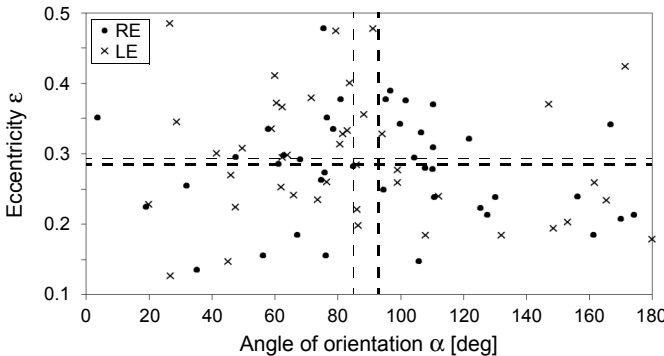

Fig. 8. The dependence of the eccentricity ε and the orientation angle α for the right and left eyes (the dashed lines represent the average value of each of the values for RE and LE).

the left eye. Thus, the orientation of the axis angle α is independent of the value of the eccentricity ε of the ellipse matched to the pupil of the eye.

4. Discussion

Obtained results show that the average size of the eye pupil in the measured group was 26.24 ± 8.90 mm^2, however it ranged from 9.68 to 48.26 mm^2.

According to WINN *et al*. [5], the pupil diameter [mm] decreases with the age A as the function $y = -0.043A + 6.046$, at constant luminance 9 cd/m^2. In our case, the dependence between the area S and the age A can be approximated with the linear function $S = -0.378A + 47.0$. Assuming the circular pupil and recalculating its area into the diameter D, this approximation can be given as the function $D = -0.0419A + 7.998$ (see Fig. 5). These results are quite similar to Winn's results, emphasizing the luminance in our examinations was about 2 cd/m^2.

The average parameter of the eccentricity ε was about 0.285. Statistical analysis showed that the differences in the right and the left eye eccentricities ε_L and ε_R are not statistically significant.

The angle α (in the range from 0 to 180 degrees, according to the scale TABO) varied in the whole range, however the mean value is quite close to the vertical axis (orientations of the long axis of the ellipse are almost vertical). The average value of α_L and α_R are statistically equal. However, the mean value of α_L was 85 degrees, while for α_R equal 93 degrees. This means that statistically the major axes of the ellipse of both eyes crosses below the head.

Since we recorded the images of the pupil through the cornea, the form of the pupil image can be deformed by the corneal astigmatism. In our examinations, the corneal astigmatism was not measured, and we cannot estimate how much the corneal astigmatism influences the eccentricity and orientation of the major axis of the elliptic approximation of the eye pupil. However, SZCZĘSNA and KASPRZAK [2] showed that values of the image eccentricity of the round pupil, observed through the cornea with astigmatism equal to 1.75 D, is smaller than 0.1 (see Table 1 in [2]). So, one can conclude that the corneal astigmatism is unlikely to be responsible for the pupil image eccentricity of order 0.2–0.4, obtained in our study.

References

[1] WILDES R.P., *Iris recognition: an emerging biometric technology*, Proceedings of the IEEE **85**(9), 1997, pp. 1348–1363.

[2] SZCZĘSNA D.H., KASPRZAK H.T., *The modeling of the influence of a corneal geometry on the pupil image of the human eye*, Optik – International Journal for Light and Electron Optics **117**(7), 2006, pp. 341–347.

[3] BOUMA H., BAGHUIS L.C.J., *Hippus of the pupil: Periods of slow oscillations of unknown origin*, Vision Research **11**(11), 1971, pp. 1345–1351.

[4] Brebbia C.A., Eglite M., Knets I., Miftahof R., Popov V., [Eds.], *Environmental Health and Biomedicine*, WIT Press, Great Britan, 2011.

[5] Winn B., Whitaker D., Elliott D.B., Phillips N.J., *Factors affecting light-adapted pupil size in normal human subjects*, Investigative Ophthalmology and Visual Science **35**(3), 1994, pp. 1132–1137.

[6] Bitsios P., Prettyman R., Szabati E., *Changes in autonomic function with age: a study of pupillary kinetics in healthy young and old people*, Age Ageing **25**(6), 1996, pp. 432–438.

[7] Merritt S.L., Schnyders H.C., Patel M., Basner R.C., O'Neill W., *Pupil staging and EEG measurement of sleepiness*, International Journal of Psychophysiology **52**(1), 2004, pp. 97–112.

[8] Barvais L., Engelman E., Eba J.M., Coussaert E., Cantraine F., Kenny G.N., *Effect site concentrations of remifentanil and pupil response to noxious stimulation*, British Journal of Anaesthesia **91**(3), 2003, pp. 347–352.

[9] Chapman C.R., Oka S., Bradshaw D.H., Jacobson R.C., Donaldson G.W., *Phasic pupil dilation response to noxious stimulation in normal volunteers: relationship to brain evoked potentials and pain report*, Psychophysiology **36**(1), 1999, pp. 44–52.

[10] Fliegert F., Kurth B., Göhler K., *The effects of tramadol on static and dynamic pupillometry in healthy subjects – the relationship between pharmacodynamics, pharmacokinetics and CYP2D6 metaboliser status*, European Journal of Clinical Pharmacology **61**(4), 2005, pp. 257–266.

[11] Knaggs R.D., Crighton I.M., Cobby T.F., Fletcher A.J., Hobbs G.J., *The pupillary effects of intravenous morphine, codeine, and tramadol in volunteers*, Anesthesia and Analgesia **99**(1), 2004, pp. 108–112.

[12] Osman E.A., Al-Saleh A.A., *Immediate changes in pupil size following laser* in situ *keratomileusis (LASIK): pupillometry study*, Saudi Journal of Ophthalmology **24**(4), 2010, pp. 139–141.

[13] Helgesen A., Hjortdal J., Ehlers N., *Pupil size and night vision disturbances after LASIK for myopia*, Acta Ophthalmologica Scandinavica **82**(4), 2004, pp. 454–460.

[14] Nowak W., Hachoł A., Kasprzak H., *Time-frequency analysis of spontaneous fluctuation of the pupil size of the human eye*, Optica Applicata **38**(2), 2008, pp. 469–480.

[15] Meeker M., Du R., Bacchetti P., Privitera C.M., Larson M.D., Holland M.C., Manley G., *Pupil examination: validity and clinical utility of an automated pupillometer*, Journal of Neuroscience Nursing **37**(1), 2005, pp. 34–40.

[16] Olson E.J., Boeve B.F., Silber M.H., *Rapid eye movement sleep behaviour disorder: demographic, clinical and laboratory findings in 93 cases*, Brain **123**(2), 2000, pp. 331–339.

[17] Iranzo A., Molinuevo J.L., Santamaria J., Serradell M., Marti M.J., Valldeoriola F., Tolosa E., *Rapid-eye-movement sleep behaviour disorder as an early marker for a neurodegenerative disorder: a descriptive study*, The Lancet Neurology **5**(7), 2006, pp. 572–577.

[18] De Santis A., Iacoviello D., *Optimal segmentation of pupillometric images for estimating pupil shape parameters*, Computer Methods and Programs in Biomedicine **84**(2–3), 2006, pp. 174–187.

[19] Calcagnini G., Lino S., Censi F., Calcagnini G., Cerutti S., *Cardiovascular autonomic rhythms in spontaneous pupil fluctuations*, Computers in Cardiology **24**, 1997, pp. 133–136.

[20] Wyatt, H.J., *The form of the human pupil*, Vision Research **35**(14), 1995, pp. 2021–2036.

[21] Sung-Sub Song, Jong-Soo Choi, Jin-Tae Kim, *Pupil extraction and tracking for interactive optical see-through HMD*, Procedia Engineering **29**, 2012, pp. 3530–3536.

[22] Roig A.B., Morales M., Espinosa J., Perez J., Mas D., Illueca C., *Pupil detection and tracking for analysis of fixational eye micromovements*, Optik – International Journal for Light and Electron Optics **123**(1), 2012, pp. 11–15.

[23] Szmigiel M.A., Kasprzak H., *Numerical analysis of variability of the eye pupil geometry based on the fast video recording*, Proceedings of SPIE **8697**, 2012, article 86970P.